

The decay of triplet pyrazine and pyrazine- D_4 in supersonic jets: Isotope effects

Israella Becker and Ori Cheshnovsky

School of Chemistry, The Sackler Faculty of Exact Sciences, Tel-Aviv University, 69978 Tel-Aviv, Israel

(Received 3 January 1994; accepted 9 May 1994)

We have measured the intersystem crossing (ISC) rates of optically excited triplet pyrazine- d_4 in supersonic expansion. ISC rates ranging from 3.3×10^2 to 1.3×10^3 were found in the 1154 cm^{-1} range of excess vibrational energy above the T_1 origin. These rates were substantially lower than the ISC rate of pyrazine. Our measurements were accompanied by model calculations of the ISC rates of pyrazine and pyrazine- d_4 . According to this model, certain vibrational modes, which undergo large frequency reduction in the excited state, regulate the strong vibrational energy dependence of the $T_1 \rightarrow S_0$ ISC of pyrazine. The large frequency changes result from the interaction of the near lying ${}^3n\pi^*$ and ${}^3\pi\pi^*$ states (the "proximity effect"). These calculations account quantitatively for the excess vibrational energy dependence of the ISC rates in pyrazine, as well as for the isotopic substitutional effect.

I. INTRODUCTION

The $T_1 \rightarrow S_0$ ISC rates of the beam isolated pyrazine in the $0\text{--}1760 \text{ cm}^{-1}$ excess energy above the T_1 origin have been recently reported by Sneh and Cheshnovsky.¹ Decay rates between $5.4 \times 10^2\text{--}1 \times 10^5 \text{ s}^{-1}$ were found in this energy range. Their results were satisfactorily explained by the model²⁻⁵ that ascribes the strong excess energy dependence of the ISC rates to specific vibrational modes. These modes serve as the main accepting modes in the first few thousand cm^{-1} above the T_1 origin, as their frequencies in the T_1 manifold are substantially lower than in the S_0 manifold. The Franck-Condon factors (FCF) of these modes, as well as the nonradiative (NR) rates, grow rapidly with excess vibrational energy up to a saturation in the energy of the T_1 and S_0 surface crossing.

The significant reduction of vibrational frequencies of such accepting modes in the triplet manifold is characteristic of many heteroaromatic molecules. The vibrational modes which participate in the mixing of the two closely lying $n\pi^*$ and $\pi\pi^*$ states (the triplet promoting modes) are strongly distorted.⁶⁻¹⁰ These same modes serve as the main accepting modes in the $T_1 \rightarrow S_0$ ISC processes. The above mechanism, introduced by Wassam and Lim,⁷ and named "the proximity effect," predicts that the NR dynamics is very sensitive to the energy separation between the proximate electronic states. This separation can be readily altered by electronic interaction induced by solvents or substituents.

The above ideas were recently supported by Sneh and Cheshnovsky in the measurements of the ISC rates of beam isolated methylpyrazine.¹¹ They have shown that the enhanced ISC rates over these of pyrazine are consistent with the proximity effect. The decrease in the $T_1\text{--}T_2$ energy gap caused by the methyl substitution induces even a larger frequency ratio in the accepting modes, and consequently enhances the ISC rates.

Isotopic substitution is known to be a useful tool and a most delicate probe in spectroscopy¹²⁻¹⁷ and molecular dynamics.¹⁸⁻²⁷ Replacing one isotope by another does not change the fundamental properties of the investigated mo-

lecular species, yet assists in clarifying some of the vague features of the research object. In aromatic, polyatomic molecules, it is common to replace hydrogen by its heavier isotope—the deuterium.

Amirav and co-workers²⁰ were the first to evaluate the deuterium effect on NR rates, in cold, beam isolated molecules by emission quantum yield measurements. Here, we present the first *direct* measurement of the influence of deuteration on the dynamics of the $T_1 \rightarrow S_0$ ISC process of single vibronic levels in the triplet manifold.

Using our technique of surface electron ejection by laser excited metastables (SEELEM)^{1,28-30} we have measured the long lifetimes of directly excited triplet states in the $0\text{--}1154 \text{ cm}^{-1}$ excess energy range above the T_1 origin of pyrazine- d_4 . The average lifetimes of the triplet states isoenergetic with the S_1 manifold were taken by measuring the long component of the fluorescence from laser excited S_1 states. The emerging picture is of a substantial (yet expected) moderation of the excess energy dependence of NR rates by about one order of magnitude (in comparison to the rates of pyrazine) in the first 1154 cm^{-1} above the T_1 origin.

We have accompanied these measurements with calculations of the energy dependence of ISC rates for the pyrazine and the pyrazine- d_4 following the model suggested by Sobolewski.^{3,4} These calculations present a quantitative agreement with the experimental deuteration effect in pyrazine.

II. EXPERIMENT

A detailed description of the experimental apparatus is given in previous works.^{1,29,30} Here we briefly describe the apparatus, with emphasis on the details relevant to this experiment.

Ar, He, or H_2 at $0.5\text{--}1.5$ bar were passed through solid samples of pyrazine and/or pyrazine- d_4 at $30\text{--}40^\circ\text{C}$. The mixture was expanded through a $0.25\text{--}0.6$ mm pulsed nozzle into a vacuum chamber. The supersonic expansion was skimmed 80 mm downstream into a differentially pumped chamber where the molecules were excited by a baffled laser

beam. 90 mm downstream of the skimmer, the molecular beam was further collimated into a third high vacuum chamber (10^{-7} Torr). In both laser-induced fluorescence (LIF) experiments and laser-induced phosphorescence (LIP) experiments, the emission was monitored by a photomultiplier perpendicular both to the laser and the molecular beam. In the LIF experiment the detection was performed in the second chamber right after the excitation (0.3 μ s delay), while in the LIP experiments the detection was performed in the third chamber 90–400 μ s (using H₂, He, or Ar) after the excitation, 21–95 μ s (in H₂, He, or Ar expansion) prior to the detection by SEELEM.

The efficiency of light collection in the LIP experiment was enhanced by a factor of 3, in comparison to the our previous studies, by using a concave mirror which was placed right below the molecular beam focusing the emission onto the photomultiplier cathode.

The SEELEM detector was installed, collinear with the beam, on a translation stage. This arrangement enabled us to vary the distance between the detector and the excitation zone over a range of 100–400 mm. This range was equivalent to 30–550 μ s flight times of the molecules in the beam, expanded in H₂, He, or Ar.

Detailed account of the SEELEM technique is given elsewhere.²⁹ In brief, it is based on electron ejection from low work function surfaces by electronically excited metastable molecules. The detector consists of a metallic target which is continuously coated with alkali metal vapor, originating from a small oven. Two cascaded microchannel plates detect the ejected electrons. In this study we have applied the following experimental methods:

Triplet spectroscopy: Simultaneous SEELEM and LIP spectra of pyrazine-*d*₄ were obtained in the third chamber, by recording the wavelength dependence of gated SEELEM and LIP signals. Some salient advantages of this LIP scheme were described previously.³⁰ The signals were digitized using a HAMEG-HM 205-3 digital oscilloscope and transferred to a microcomputer which also averaged the data, normalized it to the laser intensity, and controlled the excitation wavelength.

Relative pure radiative rates: t_D delay time after the laser excitation the LIP signal I_{LIP} can be expressed as

$$I_{LIP} \propto I_{ABS} k_r \exp(-kt_D) \Delta t, \quad (1)$$

where I_{ABS} is the absorption intensity, k_r is the pure radiative rate, and k is the total decay rate. The SEELEM technique detects the population of the excited triplets, and thus the SEELEM signal I_{SEELEM} is proportional to

$$I_{SEELEM} \propto I_{ABS} \exp(-kt_D) \Delta t. \quad (2)$$

Thus, the ratio of the LIP and the SEELEM signals is proportional to the pure radiative rate:¹

$$\frac{I_{LIP}}{I_{SEELEM}} \propto k_r. \quad (3)$$

The relative intensities of the LIP and the SEELEM signals were measured accurately by tuning the excitation laser

to a given transition and averaging the signals simultaneously. Every vibronic level was measured several times and the accuracy was better than 2%.

Triplet lifetime measurements: Lifetime measurements were performed by tuning the excitation wavelength to the Q branch of a given optical transition. time-of-flight (TOF) SEELEM traces were processed (averaged and integrated) by the HAMEG-HM 205-3 digital oscilloscope for several excitation-detector distances.²⁹ The integrated signals were fit to single exponential decay curves. Substantial effort was devoted to produce a well skimmed beam and to reduce any geometrical effects, at various nozzle-detector distances, on the detection sensitivity.

The T_1 origin lifetime of pyrazine-*d*₄ was measured in two different expansion gases. The experiment generated two different time scales in the flight tube due to different gas velocities. The measurements yielded identical lifetimes, demonstrating the absence of discernible geometrical effects on the decay lifetime measurement.

LIF spectroscopy: The total fluorescence was monitored as a function of the laser wavelength. The LIF signal was digitized by a HAMEG HM-205 digital oscilloscope and processed by a microcomputer.

LIF lifetimes: Measurements were taken with a head-on photomultiplier (perpendicular to the molecular beam and the exciting laser) in the second chamber. The transient fluorescence was averaged by a signal averager (LeCroy 9400).

III. THE CALCULATIONS OF NR RATES

The idea that frequency changes induced by the proximity effect dramatically influence the excess energy dependence of ISC rates, was advanced by Hornburger *et al.*² Sobolewski⁴ has addressed this idea with a detailed calculation, generating the excess energy dependence of ISC rates in pyrazine. For the calculation he has used all the known vibrational frequencies of pyrazine in its ground (S_0) and excited (T_1) states. In the calculation, it was assumed that prior to the ISC, rapid IVR processes partitions the energy between all the possible combinations which fit this specific excess energy. IVR has not been observed in the first 1500 cm^{-1} of electronically excited singlet states during their radiative lifetime. In triplet states however (with radiative lifetimes exceeding μ s), the assumption of complete IVR makes sense, and indeed has also been employed in treatments of the ISC process.²⁻⁵ The lack of mode specificity in the NR rates in our experiment, namely its general smooth evolution, supports this conjecture.

We have followed Sobolewski's approach and calculated NR decay rates for both the pyrazine and pyrazine-*d*₄. The reader is referred to Ref. 4 for details.

We should emphasize several technical modifications in our calculations with respect to the original procedure:⁴ the FCFs were evaluated according to Refs. 31 and 32, the grain size for the frequencies of the normal modes (a parameter defined in Ref. 4) was refined to 4 cm^{-1} (instead of 25 cm^{-1} in Ref. 4). We have used *all* the vibrational frequencies³³ and the geometry shifts,⁷ and the density of states counting procedure was the one developed by Bayer and Swinehart³⁴ for harmonic oscillators instead of the extended algorithm of

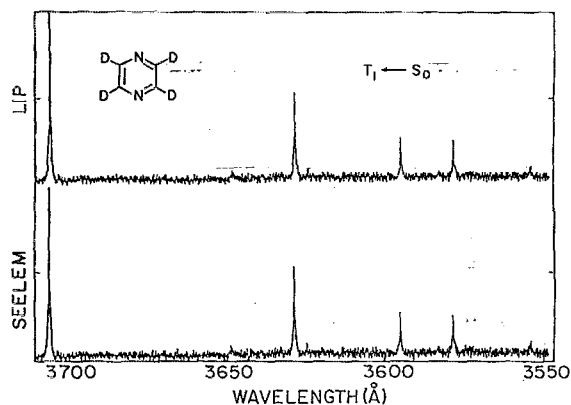


FIG. 1. Simultaneous LIP (top) and SEELEM (bottom) spectra of pyrazine- d_4 excited at $0-1154\text{ cm}^{-1}$ above the T_1 origin. 0.1 Torr of pyrazine- d_4 (at $30\text{ }^\circ\text{C}$) was expanded in 1.1 bar of H_2 through a 0.4 mm nozzle heated to $100\text{ }^\circ\text{C}$. The spectra were taken at 76 and $95\text{ }\mu\text{s}$ delay after the excitation, respectively.

Stein and Rabinovitch³⁴ for anharmonic oscillators. These modifications may explain minor differences between our results and those of Sobolewski in the simulated ISC rates of pyrazine.

IV. RESULTS

A. Vibronic spectroscopy

Excitation spectra of the $T_1 \leftarrow S_0$ manifold in the excess vibrational energy range of 1344 cm^{-1} of pyrazine- d_4 are displayed in Fig. 1. The main spectral features are similar to those observed by Fischer³⁵ in low pressure absorption experiments. Both spectra, LIP and SEELEM, were taken almost simultaneously—70 and $89\text{ }\mu\text{s}$, respectively, after the excitation. The total lifetimes of *all* the various spectral lines are extremely long (ranging from a few hundred μs to more than 2 ms) relative to the above difference between the TOFs. Therefore, these spectra can be regarded as taken simultaneously. The relative intensities of the SEELEM and the LIP spectra are practically equal and are very close to the values reported by Fisher.³⁵

B. Relative pure radiative lifetimes

The ratio between the LIP and the SEELEM signals is proportional to the pure radiative rate.³⁰ By measuring this ratio we have found that the pure radiative lifetimes of the triplet pyrazine- d_4 is practically constant over the whole energy range measured in our experiment. Using the same method, we have also found that the pure radiative lifetime of pyrazine- d_4 and pyrazine are identical within our experimental error.

C. Triplet lifetime measurements

Seven prominent spectral features on the $T_1 \rightarrow S_0$ spectrum of pyrazine- d_4 over the excess vibrational energy range of $0-1154\text{ cm}^{-1}$ are displayed in Fig. 2, and the best single exponential fits and their accuracies are summarized in Table I. Previously reported¹ lifetimes of $T_1 \rightarrow S_0$ spectral features

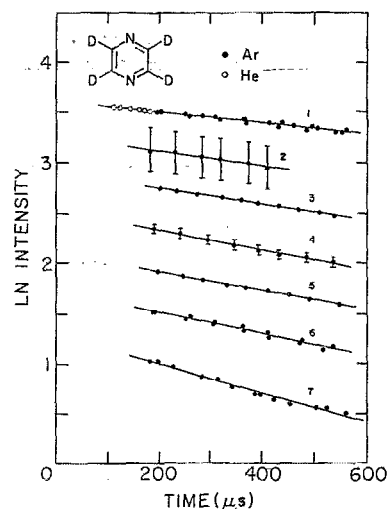


FIG. 2. Decay curves of seven prominent pyrazine- d_4 T_1 spectral features and the best fitted exponential decay lifetime: (1) $3706\text{ }\text{\AA}$, $\tau=2300\text{ }\mu\text{s}$; (2) $3649\text{ }\text{\AA}$, $\tau=1500\text{ }\mu\text{s}$; (3) $3629\text{ }\text{\AA}$, $\tau=1300\text{ }\mu\text{s}$; (4) $3621\text{ }\text{\AA}$, $\tau=1050\text{ }\mu\text{s}$; (5) $3595\text{ }\text{\AA}$, $\tau=1020\text{ }\mu\text{s}$; (6) $3579\text{ }\text{\AA}$, $\tau=940\text{ }\mu\text{s}$; (7) $3554\text{ }\text{\AA}$, $\tau=700\text{ }\mu\text{s}$. Typical error bars for long lifetimes and weak spectral features ($3649\text{ }\text{\AA}$), and for stronger peaks and shorter lifetimes ($3621\text{ }\text{\AA}$), are provided.

of pyrazine over the excess vibrational energy range of $0-1760\text{ cm}^{-1}$ are summarized in Table II. Each state has been measured several times, with special attention to prevent nonlinearities and sensitivity drifts. The decay times showed no collisional effect at several pressures of Ar, He, or H_2 .³⁶

D. LIF lifetimes

The decay of the S_1 states of pyrazine is known to be biexponential.³⁷⁻³⁹ The short component reflects the dephasing of an excited “intermediate level structure” bundle of $S_1 + \{T\}$ states.³⁷⁻⁴⁰ The ratio of the short to long components is rotational (J) dependent and is about 1.0 on top of the Q branch of pyrazine $S_1(0-0)$ at a rotational temperature of 10 K (excited by a few ns pulsed laser). Its value is around 10 in the origin of pyrazine- d_4 .^{37,41} The increase in

TABLE I. Lifetimes of vibronic levels and corrected ISC rates of pyrazine- d_4 in the 1154 cm^{-1} excess vibrational energy of the T_1 manifold.

Wave-length (Å)	Excess vib. energy (cm^{-1}) ^a	Relative intensity (%) ^b	Relative intensity (%) ^c	τ_T (μs)	k_T (s^{-1})	k_{ISC} (s^{-1}) ^d
3706	0	100	100	2300 ± 1000	4.3×10^2	3.3×10^2
3649	421	5 ± 1	5 ± 1	1500 ± 500	6.6×10^2	5.6×10^2
3629	572	49 ± 5	47 ± 5	1300 ± 450	7.6×10^2	6.6×10^2
3621	633	5 ± 1	4 ± 1	1050 ± 250	9.5×10^2	8.5×10^2
3595	833	19 ± 2	18 ± 2	1020 ± 200	9.8×10^2	8.8×10^2
3579	957	20 ± 2	18 ± 2	940 ± 200	1.1×10^3	1.0×10^3
3554	1154	4 ± 1	4 ± 1	700 ± 150	1.4×10^3	1.3×10^3

^aAbove the T_1 origin.

^bFrom delayed LIP measurements.

^cFrom SEELEM measurements.

^d $k_{\text{ISC}} = (k_T - k_r)$; $\tau_r = 10\text{ ms}$.

TABLE II. Lifetimes of vibronic levels and corrected ISC rates of pyrazine in the 1800 cm^{-1} excess vibrational energy of the T_1 manifold (raw data from Ref. 1).

Wavelength (Å)	Excess vib. energy (cm^{-1}) ^a	Relative intensity (%) ^b	Relative intensity (%) ^c	τ_T (μs)	k_T (s^{-1})	k_{ISC} (s^{-1}) ^d
3727	0	100	100	1850 ± 650	5.4×10^2	4.6×10^2
3663	437	10 ± 2	9 ± 2	1200 ± 400	8.3×10^2	7.5×10^2
3643	620	45 ± 5	48 ± 5	1000 ± 250	1.0×10^3	9.2×10^2
3596	980	9 ± 2	7 ± 2	620 ± 150	1.6×10^3	1.5×10^3
3588	1045	4 ± 1	4 ± 1	430 ± 100	2.3×10^3	2.2×10^3
3574	1145	21 ± 2	22 ± 2	200 ± 10	5.0×10^3	4.9×10^3
3564	1220	5 ± 1	5 ± 2	165 ± 30	6.1×10^3	6.0×10^3
3536	1453	<1	<1	21 ± 2	4.7×10^4	4.7×10^4
3535	1455	<1	<1	40_{-10}^{+30}	2.5×10^4	2.5×10^4
3522	1560	<1	<1	24 ± 3	4.2×10^4	4.2×10^4
3514	1626	<1	<1	16 ± 2	6.3×10^4	6.3×10^4
3499	1745	<1	<1	9 ± 2	1.1×10^5	1.1×10^5
3497	1760	<1	<1	10 ± 2	1.0×10^5	1.0×10^5

^aAbove the T_1 origin.^bFrom zero delay LIP measurements.^cFrom SEELEM measurements, lifetime corrected.^d $k_{\text{ISC}} = (k_T - k_r)$; $\tau_r = 13\text{ ms}$.

that ratio is consistent with the expected increase in the density of states due to the decrease in the frequencies of all modes due to the higher mass of deuterium.

The S_1 fluorescence lifetime of the long component in pyrazine is close to the triplet lifetime measured by the delayed ionization technique.⁴² The pure radiative lifetime of pyrazine is about 160 ns .⁴³ Diluted to 130 states³³ at the S_1 origin, the average pure radiative lifetime of each state is thus about $20\ \mu\text{s}$ and is negligible compared to the 350 ns which is the NR decay lifetime of the triplet manifold.³⁹ The pure radiative lifetimes of pyrazine- d_4 and pyrazine at S_1 are practically identical,⁴³ but due to the larger density of states (365 states³³), the diluted pure radiative lifetime of the mixed states may increase in pyrazine- d_4 to almost $60\ \mu\text{s}$.⁴⁴ The practical conclusion of this discussion is that, in view of the estimated pure radiative lifetime, we can use the emission of the long component as a probe for the much faster $T_1 \rightarrow S_0$ NR decay.¹¹

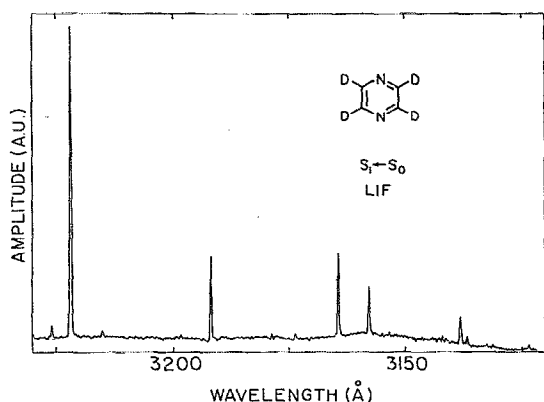


FIG. 3. LIF spectrum of pyrazine- d_4 excited at the first $0-1230\text{ cm}^{-1}$ above the S_1 origin. The 1 bar Ar seeded beam was excited 10 mm downstream the nozzle.

Figure 3 displays the laser excitation spectrum of the singlet manifold of the pyrazine- d_4 . The long component emission decay rates of the six most intense lines were measured. Figure 4 displays the emission decay of the pyrazine- d_4 $S_1(0-0)$. The decay fits well a single exponential decay of $1100 \pm 10\text{ ns}$. This value is in good correspondence with the one measured by Ohta and Takemura²² at zero magnetic field. These triplet lifetimes, measured by the excitation to the S_1 manifold, are summarized in Table III.

V. DISCUSSION

A. Isotope effect on the ISC rates

Notice that we have measured the total decay rates, while our prime interest is in the ISC decay rates. It was

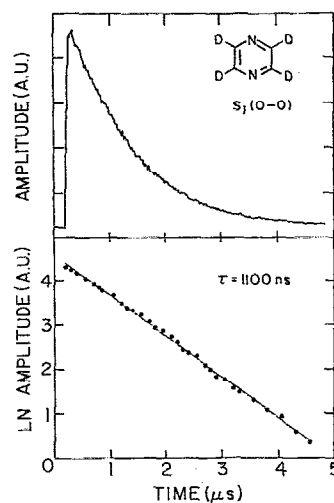


FIG. 4. The decay curve of the fluorescence long component of excited pyrazine- d_4 $S_1(0-0)$ (top). A 1100 ns single exponential decay fit of the long component fluorescence intensity (bottom). The 100 ns time constant of the amplifier completely smeared out the short component.

TABLE III. Lifetimes of vibronic levels of pyrazine- d_4 in the 1000 cm^{-1} excess vibrational energy of the S_1 manifold.

Wavelength (Å)	Excess vib. energy (cm^{-1}) ^a	τ_T (ns)
3223	0 ^b	1100 ± 10
3192	301	800 ± 20
3164	579	790 ± 15
3157	648	700 ± 20
3138	840	580 ± 30
3123	993	520 ± 35

^aAbove the S_1 origin.^b 4043 cm^{-1} above the T_1 origin.

found that the pure radiative lifetime of pyrazine T_1 excitations is constant over the ascribed range.¹ Since the pure radiative lifetime is expected to be $\sim 13\text{ ms}$ (6.5 ms in cold matrices,²³ corrected to vacuum⁴⁵) for pyrazine, it is obvious that the excess energy dependence of the decay rates practically represents the dynamics of the NR decay. The pure radiative rate is estimated to be less than 20% of the rate at the T_1 origin, and is negligible above $E_v = 1145\text{ cm}^{-1}$. This situation is not valid for pyrazine- d_4 . Its radiative rate of $\sim 10\text{ ms}$ (5 ms in cold matrices,²³ corrected to vacuum⁴⁵) is also constant over the range (Sec. IV B). However, the radiative rate is a substantial fraction of the total decay rates, even at 1000 cm^{-1} above the T_1 origin, and should not be neglected. We have evaluated the ISC rates of pyrazine- d_4 by subtracting the estimated radiative rates from the total decay rates. These values are listed in Table I. Table II presents the slightly reevaluated ISC rates of pyrazine.¹

Figure 5 displays the excess energy dependence of the corrected ISC rates of cold isolated pyrazine¹ and pyrazine- d_4 molecules. The full squares correspond to pyrazine, while the open squares correspond to pyrazine- d_4 . The

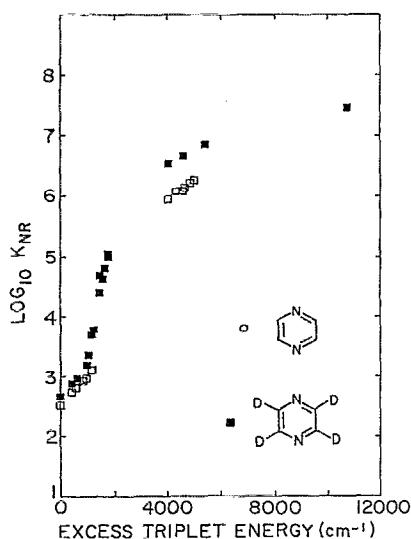


FIG. 5. Corrected ISC decay rates of pyrazine (full squares) and pyrazine- d_4 (hollow squares) plotted as a function of excess vibrational energy above the T_1 origin. Data for pyrazine with excess vibrational energy over 4000 cm^{-1} were taken from Ref. 42.

TABLE IV. The energy gaps (cm^{-1}) between the various electronic manifolds of pyrazine and pyrazine- d_4 in isolated molecules.

	$S_0-T_1^a$	$T_1-T_2^b$	$T_1-S_1^a$
Pyrazine	26 831	≈ 1500	4056
Pyrazine- d_4	26 976	≈ 1500	4043

^aFrom our measurements.^bReference 7.

four high energy full squares are the results of Dietz *et al.*,⁴² who examined the indirectly excited triplet states above the S_1 origin, while the others are our results for directly excited T_1 states (Table II). The decay rates of pyrazine- d_4 combine our SEELEM measurements of directly excited triplets (Table I) and the LIF long components decay rates (Table III). It is clear from Fig. 5 that the deuterium substitution moderates the nonradiative decay rates of the T_1 state, with respect to pyrazine.

The electronic energy level structure and gaps of the perdeuterated species are identical with that of the perprotonated one (Table IV). It has also been argued and calculated⁷ that the T_1-T_2 vibronic interaction coupling term is isotopically invariant so that the ratio of the T_1 to S_0 force constants should be the same for both species. As the ratio is equal, the difference in frequencies should be smaller for pyrazine- d_4 than for pyrazine. Thus, deuteration of the vibronically active C-H group will lead to a significant reduction of the FCF and hence, to a decrease of the NR rates. On the other hand, this effect will be compensated by the increase in the density of states of the accepting modes, leading to a relatively small total change in the NR rates.

The simulated ISC rates for pyrazine and pyrazine- d_4 are presented in Fig. 6 as full and dashed lines, respectively.

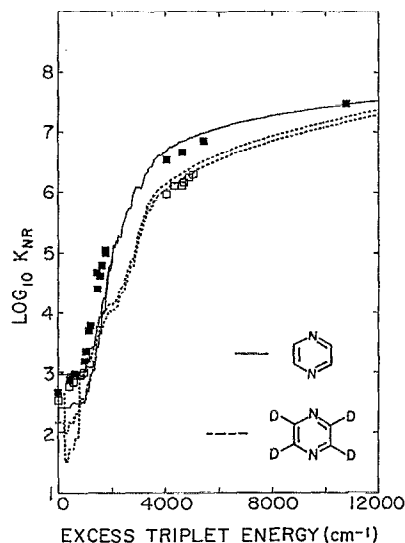


FIG. 6. Model simulation of the experimental ISC rates. The solid lines represent the simulation for pyrazine, with geometry shifts of 0.2 (bottom solid line) and 0.3 (top solid line). The dashed lines represent the simulation for pyrazine- d_4 with, geometry shifts of 0.1 (bottom dashed line) and 0.15 (top dashed line).

TABLE V. Frequency and geometry shift values used for the Sobolewski algorithm, taken from Ref. 7.

Vib. mode	Pyrazine		Pyrazine- d_4	
	Frequency (cm ⁻¹)		Frequency (cm ⁻¹)	
	T_1	S_0	T_1	S_0
ν_{10a}	398	919	303	726
ν_5	350	757	277	590
	Geometry shift (Δ)		Geometry shift (Δ)	
	0.2–0.3		0.1–0.15	

Both calculations, for pyrazine and pyrazine- d_4 , were scaled with the same arbitrary spin-orbit coupling factor (10^9 Hz) to fit the experimental results. The frequency and geometry shift values, as summarized in Table V, were used for the excess energy dependence calculation.

This simulation reproduced well the excess energy dependence as well as the deuteration effect of pyrazine. Together with previous results of the ISC in methylpyrazine,¹¹ it provides a strong support for the validity of the proximity effect, namely the important role of the $n\pi^* - \pi\pi^*$ interaction on the photodynamics of heteroaromatic molecules.

B. The pure radiative lifetime

Deuterium isotope effects on electronic transition can arise either from the FCF and/or from the electronic matrix elements. As discussed earlier, in nonradiative transition, the deuteration effect on the Franck-Condon factor dominates. For radiative transitions, however, the Franck-Condon factor dictates only the distribution of intensity among the 0–0 transition and the transitions to the excited vibrational levels of the final electronic state. It has no overall influence on the final integrated intensity.³⁵ Thus, any deuteration effect on the above radiative transition must be largely due to an effect on the electronic matrix element.

EPR⁴⁶ and fluorescence/phosphorescence⁴⁷ measurements proved that deuterium substitution has no influence on the radiative transition probability from the zero vibrational level of T_1 to the ground state S_0 for both naphthalene⁴⁶ and benzene.⁴⁷ Our k_r measurements (Sec. IV B) of the T_1 manifolds of pyrazine and pyrazine- d_4 indicate that the pure radiative rates are equal and practically constant over a wide excess vibrational energy of the two manifolds.

In a previous publication,¹ Sneh and Cheshnovsky noted that the data accumulated by that time on the triplet state of isolated pyrazine did not allow them to provide a detailed explanation for the constancy of the pure radiative rate with excess vibrational energy. It allowed them, however, to speculate that the changes in the ISC rates of the triplet pyrazine do not originate from *vibronically induced* spin-orbit coupling. The reason for that is that vibronically induced spin-orbit coupling would have influenced the pure radiative lifetimes as well, contrary to their results. Fischer and Lim⁴⁸ treat this perplexity theoretically; they distinguish four mechanisms for the radiative transition: one of them is purely spin-orbit coupling, while the other three are spin-orbit couplings induced by various kinds of vibronic cou-

plings. They reach the conclusion that only the first one is not subject to any deuteration effect, while for the rest, the dependence of the partial radiative rate constant k for the mode j is given by the general rule:

$$k_j^H/k_j^D = (\omega_j^H/\omega_j^D)^n, \quad (4)$$

where ω_j is the typical frequency of mode j , and $n = 1, 3, 4$ for the second, third, and fourth mechanisms, respectively.

The equality (within experimental error) of the radiative rate constants of pyrazine and pyrazine- d_4 T_1 origins, and the lack of mode specificity *all along* the triplet manifolds rule out all three of the $T_1 - S_0$ vibronic coupling dependent mechanisms and adopts the pure spin-orbit one. By comparing the radiative rates of those two isotopically variant structures, we have strengthened the attribution of pure spin-orbit coupling in pyrazine.

VI. CONCLUSIONS

We have shown that the isotopic effect on the NR rates of the ISC process in pyrazine can be quantitatively explained by using the spectroscopic data on the S_0 and $T_1(n\pi^*)$ states of pyrazine. A large frequency reduction of the accepting modes in the T_1 manifolds of both compounds [due to interaction of the proximate $T_1(n\pi^*)$ and $T_2(\pi\pi^*)$] is the main factor determining the functional dependence of the $T_1 \rightarrow S_0$ ISC rate.

This picture is consistent with the ISC rates of methylpyrazine previously reported by this laboratory¹¹ and strongly supports the proximity effect model, advanced by Wassam and Lim,⁷ in order to explain the photodynamics of heteroaromatic molecules.

ACKNOWLEDGMENTS

We thank Bruce Weisman for supplying us with the pyrazine- d_4 , and both Ofer Sneh and Aviv Amirav for stimulating discussions. This research was supported by the Fund for Basic Research, administrated for the Israel Academy of Sciences and Humanities, and the James-Franck German-Israeli Binational program in Laser-Matter Interactions.

¹O. Sneh, D. Dunn-Kittenplon, and O. Cheshnovsky, *J. Chem. Phys.* **91**, 7331 (1989).

²H. Hornburger, H. Kono, and S. H. Lin, *J. Chem. Phys.* **81**, 3554 (1984).

³A. L. Sobolewski and J. Prochorow, *Chem. Phys.* **92**, 211 (1985).

⁴A. L. Sobolewski, *Chem. Phys.* **115**, 469 (1987).

⁵H. Kono, S. H. Lin, and E. W. Schlag, *Chem. Phys. Lett.* **145**, 280 (1988).

⁶E. C. Lim, in *Excited States*, edited by E. C. Lim (Academic, New York, 1977), Vol. III.

⁷W. A. Wassam and E. C. Lim, *J. Chem. Phys.* **68**, 433 (1978).

⁸A. J. Duben, L. Goodman, and M. Koyangi, in *Excited States*, edited by E. C. Lim (Academic, New York, 1977), Vol. I.

⁹R. M. Hochstrasser and C. Marzocco, *J. Chem. Phys.* **49**, 971 (1968).

¹⁰K. Kanamaru and E. C. Lim, *J. Chem. Phys.* **62**, 3252 (1975).

¹¹O. Sneh and O. Cheshnovsky, *J. Chem. Phys.* **96**, 8095 (1992).

¹²H. Hong and G. W. Robinson, *J. Mol. Spectrosc.* **52**, 1 (1974).

¹³S. N. Thakur and K. K. Innes, *J. Mol. Spectrosc.* **52**, 130 (1974).

¹⁴D. L. Narva and D. S. McClure, *Chem. Phys.* **11**, 151 (1975).

¹⁵N. Nishi, M. Kinoshita, T. Nakashima, R. Shimada, and Y. Kanda, *Mol. Phys.* **33**, 31 (1977).

¹⁶I. Suzuka, Y. Udagawa, and M. Ito, *Chem. Phys. Lett.* **64**, 333 (1979).

- ¹⁷W. R. Lambert, P. M. Felker, J. A. Syage, and A. H. Zewail, *J. Chem. Phys.* **81**, 2195 (1984).
- ¹⁸I. Yamazaki, M. Fujita, and H. Baba, *Chem. Phys.* **57**, 431 (1981).
- ¹⁹I. Yamazaki, T. Mura, and K. Yoshihara, *Chem. Phys. Lett.* **87**, 384 (1982).
- ²⁰A. Amirav, M. Sonnenschein, and J. Jortner, *Chem. Phys. Lett.* **100**, 488 (1983).
- ²¹J. L. Knee and C. E. Otis, *J. Chem. Phys.* **81**, 4455 (1984).
- ²²N. Ohta and T. Takemura, *J. Chem. Phys.* **95**, 7133 (1991).
- ²³D. M. Buralnd and J. Schmidt, *Mol. Phys.* **22**, 19 (1971).
- ²⁴S. H. Lin and R. Bersohn, *J. Chem. Phys.* **48**, 2732 (1968).
- ²⁵C. A. Hutchinson, Jr. and B. W. Magnum, *J. Chem. Phys.* **32**, 1261 (1960).
- ²⁶W. Siebrand, *J. Chem. Phys.* **46**, 440 (1967).
- ²⁷J. P. Byrne, E. F. McCoy, and I. G. Ross, *Aust. J. Chem.* **18**, 1589 (1965).
- ²⁸O. Sneh and O. Cheshnovsky, *Chem. Phys. Lett.* **130**, 53 (1986).
- ²⁹O. Sneh and O. Cheshnovsky, *J. Isr. Chem. Soc.* **30**, 13 (1990).
- ³⁰O. Sneh and O. Cheshnovsky, *J. Phys. Chem.* **95**, 7154 (1991).
- ³¹W. M. Gelbert, K. G. Spears, K. F. Freed, J. Jortner, and S. A. Rice, *Chem. Phys. Lett.* **6**, 345 (1970).
- ³²M. C. Prais, D. F. Heller, and K. F. Freed, *Chem. Phys.* **6**, 331 (1974).
- ³³P. M. Felker and A. H. Zewail, *Chem. Phys. Lett.* **128**, 221 (1986).
- ³⁴S. E. Stein and B. S. Rabinovitch, *J. Chem. Phys.* **58**, 2438 (1973).
- ³⁵G. Fischer, *Chem. Phys. Lett.* **79**, 573 (1981).
- ³⁶Note that in the microsecond and millisecond time scale intrabeam collisions and background pressure (10^{-7} Torr) collisions may influence the lifetime.
- ³⁷J. Kommandeur, W. A. Majewski, W. L. Meerts, and D. W. Pratt, *Annu. Rev. Phys. Chem.* **38**, 433 (1987).
- ³⁸A. Frad, F. Lahmani, A. Tramer, and C. Tric, *J. Chem. Phys.* **60**, 4419 (1974).
- ³⁹A. Amirav, *Chem. Phys.* **108**, 403 (1986).
- ⁴⁰M. Bixon and J. Jortner, *J. Chem. Phys.* **48**, 715 (1967).
- ⁴¹B. J. van der Meer, H. Th. Jonkman, G. M. ter Horst, and J. Kommandeur, *J. Chem. Phys.* **76**, 2099 (1982).
- ⁴²T. G. Dietz, M. A. Duncan, A. C. Pulu, and R. E. Smalley, *J. Phys. Chem.* **86**, 4026 (1982).
- ⁴³S. L. Madej, G. D. Gillispie, and E. C. Lim, *Chem. Phys.* **32**, 1 (1978).
- ⁴⁴This is an upper limit for the pure radiative lifetime, assuming complete dilution of the oscillator strength of the singlet in the background triplet states over the coupling width. The resulting lifetime is orders of magnitude larger than necessary to consider the measured lifetime as the NR rate only.
- ⁴⁵A. B. Myers and R. R. Birge, *J. Chem. Phys.* **73**, 5314 (1980).
- ⁴⁶M. S. de Groot and J. H. van der Waals, *Mol. Phys.* **4**, 189 (1961).
- ⁴⁷E. C. Lim and J. D. Laposa, *J. Chem. Phys.* **41**, 3257 (1964).
- ⁴⁸S. F. Fischer and E. C. Lim, *Chem. Phys. Lett.* **14**, 40 (1972).